Food and Chemical Toxicology 126 (2019) 285–294

Contents lists available at ScienceDirect

Food and Chemical Toxicology

journal homepage: www.elsevier.com/locate/foodchemtox

Development and application of a population physiologically based pharmacokinetic model for florfenicol and its metabolite florfenicol amine in cattle

Fan Yang[a,b], Zhoumeng Lin[c], Jim E. Riviere[a], Ronald E. Baynes[a,*]

[a] Department of Population Health and Pathobiology, Center for Chemical Toxicology and Research Pharmacokinetics, North Carolina State University, College of Veterinary Medicine, Raleigh, NC, United States
[b] College of Animal Science and Technology, Henan University of Science and Technology, Luoyang, 471023, China
[c] Institute of Computational Comparative Medicine (ICCM), Department of Anatomy and Physiology, College of Veterinary Medicine, Kansas State University, Manhattan, KS, 66506, United States

ARTICLE INFO

Keywords:
Physiologically based pharmacokinetic (PBPK) model
Withdrawal interval
Florfenicol
Florfenicol amine
Cattle

ABSTRACT

Florfenicol (FF) is used in cattle to treat respiratory diseases but could result in tissue residues. This study aimed to develop a population physiologically based pharmacokinetic (PBPK) model to predict the concentrations of FF and its metabolite, florfenicol amine (FFA), in cattle after four different routes of administration, and to calculate and compare the withdrawal intervals (WDIs) with approved withdrawal times based on different marker residues and their MRLs or tolerances. A flow-limited PBPK model including both FF and FFA sub-models were developed with published data using acslXtreme. This model predicted FF and FFA concentrations in tissues and plasma/serum after intramuscular or subcutaneous administration. Based on the model, the WDIs of 46 and 58 days were calculated to ensure that total residue concentrations (FF + FFA) in 95th percentile of the population after intramuscular and subcutaneous administration were below the MRL, respectively. WDIs were calculated as 44 and 47 days to ensure that FFA concentrations after intramuscular and subcutaneous administration fell below tolerances in 99th percentile of the population, respectively. WDIs were longer than the corresponding label in China, US, and EU. This model provides a useful tool to predict tissue residues of FF and FFA in cattle to improve food safety.

1. Introduction

Florfenicol (FF, 2,2-dichloro-~{N}-[(1~{R},2~{S})-3-fluoro-1-hydroxy-1-(4-methylsulfonylphenyl)propan-2-yl]acetamide, $C_{12}H_{14}Cl_2FNO_4S$, CAS # 73231-34-2) is a wide spectrum, synthetic antibacterial substance and is commonly used to treat respiratory diseases in animals (Atef et al., 2010). It inhibits protein synthesis of susceptible bacteria (Gilliam et al., 2008), and acts by a concentration-dependent killing mechanism (Sidhu et al., 2014). *In vitro* studies have shown that FF has potent activity against respiratory pathogens, including *Mycoplasma bovis* (Klein et al., 2017), *Pasteurella multocida* (Wang et al., 2015; Welsh et al., 2004), *Mannheimia haemolytica* (Timsit et al., 2017; Welsh et al., 2004), and *Histophilus somni* (Klima et al., 2014; Timsit et al., 2017; Welsh et al., 2004). *In vivo* studies have also demonstrated that FF is efficacious in the treatment of bovine respiratory diseases (Hendrick et al., 2013; Lamm et al., 2012; Thiry et al., 2014).

To our knowledge, FF residue in edible tissues from cattle is relatively common compared with other antibiotics. In China, US, and the EU, FF is labeled to be subcutaneously or intramuscularly given to cattle with the same approved doses: a single subcutaneous dose at 40 mg/kg body weight (BW) or two intramuscular doses each at 20 mg/kg BW with a 48-h interval (Commission of Chinese Veterinary Pharmacopoeia (CCVP), 2015; EMA, 2002; FARAD, 2002). However, different regulatory authorities adopted different marker residues and/or withdrawal periods. In China, the marker residue of FF is the sum of parent compound and one of its metabolites, florfenicol amine (FFA, (1R,2S)-2-amino-3-fluoro-1-(4-methylsulfonylphenyl)propan-1-ol, $C_{10}H_{14}FNO_3S$, CAS # 76639-93-5), which is consistent with the marker residue used by EMA (2002). The same maximum residue limits (MRLs) for FF plus FFA of 0.2, 0.3, and 3 μg/g in muscle, kidney, and liver, respectively are used in both China and EU (CCVP, 2015; EMA, 2002),

* Corresponding author.
E-mail addresses: yfscau@126.com, fyang@haust.edu.cn (F. Yang), zhoumeng@vet.k-state.edu (Z. Lin), jim.riviere@gmail.com (J.E. Riviere), Ronald_Baynes@ncsu.edu (R.E. Baynes).

https://doi.org/10.1016/j.fct.2019.02.029
Received 31 October 2018; Received in revised form 14 February 2019; Accepted 19 February 2019
Available online 27 February 2019

while in the US, the marker residue is only FFA with the tolerances in liver and muscle being 3.7 and 0.3 μg/g, respectively (FDA, 2017). In addition to the differences in the marker residues and their MRLs or tolerances between US and the other two regions; different percentiles of population are used to calculate the withdrawal time. In China and EU, the 95th percentile is used; however, the 99th percentile is used in the US. In addition to the differences listed above, different withdrawal times were adopted by these regulatory authorities even under the same dosing regimen in cattle. In China, the labeled withdrawal time of FF is 28-day in cattle after both intramuscular and subcutaneous injections (CCVP, 2015); while in the US and EU, the labeled withdrawal times after IM injections are 28 and 30 days, respectively, and 38 and 44 days after subcutaneous injection, respectively (FARAD, 2002; Veterinary Medicines Directorate, 2007).

Excessive antibiotic residues in edible tissues may cause adverse effects on human health (Baynes et al., 2016; Li et al., 2013; Yang et al., 2013a). Their direct toxic effects include allergic reactions, carcinogenic effect, gastrointestinal disturbances, photosensitivity, etc. In addition to these direct toxic effects, consumers are more concerned about the potential prevalence of antibiotic resistance via exerting selective pressure on bacteria (Liu et al., 2017; Yang et al., 2016). Toxicity studies conducted in rats (7, 14, 28 days and 13, 52 weeks) have shown that FF caused changes in hematologic parameters, increases in liver weights, and atrophy of testes (EMA, 2002). Therefore, the residues of FF and its related compounds should be closely monitored, and it is of great importance to accurately predict their tissue residues in cattle.

In recent years, there has been an increase in the applications of physiologically based pharmacokinetic (PBPK) models to predict veterinary drug residues (Henri et al., 2017; Leavens et al., 2014; Yang et al., 2013b, 2018; Zhu et al., 2017) and their withdrawal intervals (WDIs) (Buur et al., 2006; Li et al., 2017; Lin et al., 2016; Yang et al., 2012, 2014, 2015; Zeng et al., 2017). WDIs in this manuscript are to distinguish withdrawal periods derived from PBPK modeling from approved withdrawal periods (withdrawal times, WDT) derived from regulatory authorities such as EMA in EU and US FDA in US. Compared with the traditional empirical tolerance limit method for calculating WDIs based on a single set of animal experimental data (FDA, 2018), PBPK models are predictive in nature, and are based on mass-balance equations and allow for the use of *in vitro* mechanistic as well as population variability data to be incorporated to predict the drug concentrations in edible tissues in a diverse population of animals (Lin et al., 2016). PBPK models for FF have been reported in crucian carp (Yang et al., 2013b) and pigs (Qian et al., 2017). However, the corresponding model is not available in cattle. In addition, the marker residue FFA was not incorporated in the previous two models and thus they were limited in usefulness to predict the tissue depletion kinetic profiles for FF only.

Taking into account the extensive applications of FF in cattle and its residues in edible tissues from cattle, it is of great importance to establish a PBPK model including both FF and FFA to predict their residues in cattle. The objectives of this study were (i) to develop and validate a PBPK model incorporating both FF and FFA in cattle; (ii) use this model to predict the residue concentrations and WDIs after different routes of administration; (iii) to compare the WDIs under the same dosage regimen but calculated according to the different marker residues and their tolerances or MRLs, as well as different percentiles, used by China, US, and EU.

2. Method

2.1. Concentrations versus time data of FF and FFA

All the concentrations *versus* time data of FF and FFA were obtained from the Food Animal Residue Avoidance Databank (FARAD) comparative pharmacokinetic database (http://www.farad.org; Riviere et al., 2017). The pharmacokinetic studies in cattle after intravenous (IV), oral (PO), intramuscular (IM), or subcutaneous (SC) administration were selected. The plasma, serum, or tissue concentrations of FF and FFA were obtained from the published table or extracted from the published figures using GetData Graph Digitizer (version 2.26; http://getdata-graph-digitizer.com). Key information of selected studies is given in Table S1.

2.2. Model structure

The PBPK model included two sub-models: FF and its metabolite FFA, which were connected with each other through hepatic metabolism. FF sub-model was consisted of eleven compartments, including stomach, intestine, liver, kidney, fat, muscle, lung, venous blood, arterial blood, injection site (only for IM or SC models), and a compartment representing the rest of the body (Fig. S1). Compared with FF sub-model, stomach, intestine, fat, lung, and injection site were not incorporated in the FFA sub-model, and a mixed blood compartment was used instead of venous and arterial blood (Fig. S1). As IM and SC injections are the labeled routes of administration for FF in cattle, they were both incorporated into the present FF sub-model. In addition to these two approved routes, the IV and PO routes were also included, because the IV concentration data could be used to determine the parameters related to drug elimination and distribution that would be further used under all routes of administration, while the rich PO concentration data (Adams et al., 1987; Croubels et al., 2006; Varma et al., 1986) were able to be used for further optimization or validation of this model. According to our previous model for FF in crucian carp (Yang et al., 2013b), the flow-limited compartments were applied for both FF and FFA in the current study. The software of acslXtreme (version 3.0.2.1; Aegis Technologies Group, Inc., Huntsville, Alaska) was used to develop this model and run all simulations. The model code is provided in the Supplementary Materials.

After IV administration, it was assumed that FF was directly injected into the venous blood with the IV dose (mg/kg) multiplied by BW (kg) and then divided by the duration of the infusion period (timeiv) which was set as 0.001 h according to our previous report (Yang et al., 2018).

A two-compartment model (Yang et al., 2018) was used to simulate the drug absorption after IM or SC injection. The injection site was virtually divided into two parts: injection sites 1 and 2 (abbreviated as IS1 and IS2, respectively), and it was assumed that FF was injected into both IS1 and IS2 at the same time (time zero). For IM model, drug allocated to IS1 was calculated as IM dose multiplied by F_{im1} (unitless), while the other FF was allocated to IS2 whose amount was equal to IM dose multiplied by F_{im2} (unitless), and the sum of F_{im1} and F_{im2} was 1. For SC model, similar parameters (SC dose, F_{sc1}, and F_{sc2}) were used as in the IM model. After IM or SC injection, FF was absorbed only from IS1 with the absorption rate constants of K_{aim} or K_{asc}, respectively, and drug was distributed from IS2 to IS1 with the distribution rate constants of K_{disim} or K_{dissc}, respectively (Fig. S1). The absorbed drug went directly into venous blood. To accurately simulate the absorption after IM and SC injections, the bioavailability of FF was assumed to be 80% (F_{aim}; Lobell et al., 1994) and 100% (F_{asc}; Norbrook Laboratories, Ltd., 2015), respectively. Moreover, to simplify the process of drug absorption, it was assumed that there was not any blood flow through both IS1 and IS2, and the injection site only served as a site for drug exposure and absorption. More details about the differential equations to describe the IM and SC absorptions can be found in Table S2.

After PO administration, another two-compartment model consisting of stomach and intestine was used to simulate the drug absorption according to our previous studies (Yang et al., 2013b, 2018). It was assumed that FF went directly into stomach where it was available immediately, then was transported to intestine by gastric emptying with the rate of K_{st} and eventually absorbed there. Once in intestine, FF was completely absorbed with a bioavailability of 100% (Adams et al., 1987; Varma et al., 1986), and the absorption was only controlled by the absorption rate constant of K_{apo}. The absorbed FF was assumed to

Table 1
Parameters of tissue weights, blood flows, and tissue/plasma partition coefficients used in this multiroute physiologically based pharmacokinetic model.

Compartment	FF sub-model		FFA sub-model		Partition coefficient for FF[c] (P_x)	Partition coefficient for FFA[d] (P_{mx})
	Tissue weight[a] (V_{cx}, fraction of body weight)	Blood flow[b] (Q_{cx}, fraction of cardiac output)	Tissue weight[a] (V_{cmx}, fraction of body weight)	Blood flow[b] (Q_{cmx}, fraction of cardiac output)		
Liver	0.014	0.405[e]	0.014	0.405[e]	1.3	8.7414
Kidney	0.002	0.090	0.002	0.090	0.9	1.3026
Fat	0.150	0.080	NA	NA	0.1137	NA
Lung	0.008	1	NA	NA	0.9	NA
Muscle	0.270	0.180	0.270	0.180	0.9	0.2778
Injection site (IM or SC)	5 kg[f]	NA	NA	NA	NA	NA
Arterial blood	0.010	NA	NA	NA	NA	NA
Venous blood	0.030	NA	NA	NA	NA	NA
Total blood	NA	NA	0.040[g]	NA	NA	NA
Rest	0.516[h]	0.2450[i]	0.674[j]	0.325[k]	1.1332	0.0121

Note: NA = not available.

[a] Mean body weight (BW) was different in the published articles (Table S1), so this model was adjusted according to the average BW of cattle used in the study. The parameters of tissue weights were derived from previously reported cattle model for penicillin G (Li et al., 2017).

[b] A cardiac output (CO) of 5.970 L/h/kg was reported by Doyle et al. (1960), and convert its unit from L/h/kg to L/h by the follow equation: $Q_{tot} = CO \times BW$. And the blood flow for a tissue presented here represent fraction of Q_{tot}, and their values were derived from the report by Li et al. (2017).

[c] Partition coefficient (P_x) for FF in muscle, liver, and kidney in cattle were assumed to be equal to those previously reported in fish (Yang et al., 2013b). While those in lung and fat were not reported in fish, so we optimized them.

[d] All partition coefficients (P_{mx}s) for FFA were obtained through optimization, and more details can be found in the manuscript.

[e] This value is the sum of hepatic artery plus portal vein flows.

[f] It was fixed to be 5 kg, and included in muscle fraction. In addition, the IM and SC injection sites were separated in the present model; both of them were assumed to be the source of drug exposure.

[g] Its value was equal to the sum of arterial and venous blood listed in the second column.

[h] This value was calculated as 1-(0.030 + 0.010 + 0.270 + 0.008 + 0.150 + 0.002 + 0.014).

[I] This value was calculated as 1-(0.180 + 0.080 + 0.090 + 0.405).

[j] This value was calculated as 1-(0.040 + 0.270 + 0.002 + 0.014).

[k] This value was calculated as 1-(0.405 + 0.090 + 0.180).

directly enter the liver compartment from portal vein. To simplify the PO model, portal vein was not modelled in details and it was merely a passageway for drug transport. Moreover, hepatic blood flow in this study was modelled as the combination of hepatic arterial and portal veins (Table 1). A virtual stomach compartment was used to represent a simplified model of the ruminant stomachs of cattle, with the stomach and intestine only serving as sites for drug exposure and absorption, respectively. In this model, gastric emptying and drug absorption were both assumed to be first-order processes. More details about the differential equations describing the oral absorption can be found in Table S2.

After IV injection or absorption after extravascular administration, FF is distributed to all tissue compartments through the blood flow. As previously described (Yang et al., 2012, 2013b, 2018), the mass-balance differential equations (Table S2) were used to describe the FF and FFA change rate in each compartment. According to the previous report (EMA, 2002), FF is mainly eliminated by renal excretion and liver metabolism. Therefore, the parameters of Cl_{re} and K_m were used to simulate these two processes, respectively. Cl_{re} was the abbreviation for renal clearance of FF, which was further normalized by BW and abbreviated as $Cl_{reperkg}$ in the final model, while K_m was the metabolic rate constant from FF to FFA in liver. According to the report of EMA (2002), there are some other metabolites of FF besides the main metabolite FFA, such as florfenicol alcohol, florfenicol oxamid acid, and monochloride florfenicol. Additionally, in a radiometric depletion study conducted in Atlantic Salmon after a single PO dose of 10 mg/kg BW, the ratios of FF and FFA to total radioactivity was determined as 4% and 50.7%, respectively (EMA, 1997). Therefore, in the present study, it was assumed that FFA account for 50% of all metabolites, and a parameter of FractionFFA was used to simulate this (Table S2). Since only FFA is the marker residue of FF, all other metabolites were not monitored in the present model. And the metabolic rate constants from FF to other metabolites were combined, and abbreviated as K_{mo}. FFA is also distributed to other tissues through the blood flow after its formation in liver. Because the main elimination route of FFA in cattle was via urine (63–71%; EMA, 1996), it was assumed that FFA was eliminated only by renal excretion and its renal clearance was abbreviated as Cl_m, which was also normalized by BW (abbreviated as Cl_{mperkg}). More details about the differential equations describing the eliminations of FF and FFA can be found in Table S2.

2.3. Model parameterization

It should be noted that all common parameters used in different routes of the model shared their same values. Since the previously reported concentrations in both serum and plasma (Table S1) would be used to optimize or validate the present model, the parameters of pcv (abbreviation for hematocrit) and pse were used to calculate the proportions of plasma and serum to the total volume of whole blood, respectively (more details can be found in the model code provided in the Supplementary Materials). In order to simplify the simulation, it was assumed that neither FF nor FFA would enter blood cell and the amount of each compound in blood was equal to that in serum or plasma.

The other model parameters, including tissue weight (V_{cx} or V_{cmx}), blood flow (Q_{cx} or Q_{cmx}), and the tissue/plasma partition coefficients for both FF and FFA (abbreviated as P_x and P_{mx}, respectively), are listed in Table 1. The tissue weight and blood flow were both derived from the previous model for penicillin G in cattle (Li et al., 2017), and expressed as the fractions of BW and cardiac output (CO), respectively. Because the average BWs of cattle were different in the previously published studies (Table S1), the present model was adjusted according to the specific BW reported in each study. The value of CO was 5.970 L/h/kg (Doyle et al., 1960), and its unit was converted to L/h using the following equation: $Q_{tot} = CO \times BW$. The values of P_xs in muscle, liver, and kidney were assumed to be equal to those previously reported in fish (Yang et al., 2013b). While those values in lung, fat, and rest of

body compartment, which were not available in our previous fish model, were obtained by optimization using the serum concentration data reported by Bretzlaff et al. (1987). For all P_{mx}s, their values were not available and were obtained through parameter optimization by fitting to the published tissue concentrations of FFA (Schering-Plough Animal Health Corporation, 2008). More details on the optimization process were described below.

In addition to those optimized P_xs and P_{mx}s mentioned above, there were other parameters whose values were difficult to be obtained. Therefore, we also optimized them using the published FF and/or FFA concentrations (Table S1). It should be noted that all parameter optimizations were performed in the software of acslX using a maximum likelihood algorithm of Nelder-Mead. During the parameter optimization process, the serum concentrations of FF after IV injection (Bretzlaff et al., 1987) were firstly used to optimize the parameters used in all four routes of the model. These parameters included $Cl_{reperkg}$, partition coefficients for FF in fat, lung, and rest of body (P_{fa}, P_{lu}, and P_{re}, respectively), as well as metabolic rate constants from FF to FFA (K_m) and from FF to all other metabolites (K_{mo}). The reason for choosing the study of Bretzlaff et al. (1987) to perform the first optimization was that detailed serum concentrations *versus* time data in five individuals were reported in that study, and therefore it was relatively easy to obtain the accurate optimization results. When the final values of these six parameters were obtained, the FF concentrations in plasma or serum after IV injection (Table S1) published by other researchers (Adams et al., 1987; de Craene et al., 1997; Gilliam et al., 2008; Lobell et al., 1994; Varma et al., 1986) were used to verify the validity of these parameters through visual comparisons of the predicted and published FF concentrations. If most predictions were consistent with the observations, these optimized parameter values were fixed. Next, we further optimized other parameters used in the SC model, including K_{asc}, K_{dissc}, and F_{sc1} based on the FF concentrations in plasma published by Kawalek et al. (2016). The other concentration data in plasma or serum (Lacroix et al., 2011; Schering-Plough Animal Health Corporation, 2006; Sidhu et al., 2014) were used to validate these optimized values.

After final determination of these parameter values for FF, the published tissue concentrations of FFA after SC administration (Schering-Plough Animal Health Corporation, 2008) were used to further optimize the parameters for FFA in all routes of the model. These parameters included BW-normalized clearance of FFA (Cl_{mperkg}) and all partition coefficients for FFA, including P_{mli}, P_{mki}, P_{mmu}, and P_{mre}. And the concentrations of FFA reported by others (Intervet, Inc., 2009; Norbrook Laboratories, Ltd., 2015) were used to validate these optimized values. Until now, most parameters used in this multiroute model were determined except those related to the absorption after IM and PO administration, including K_{aim}, F_{im1}, K_{disim}, K_{st}, and K_{apo}. Therefore, the previously reported FF concentrations in plasma or serum (Croubels et al., 2006; Lobell et al., 1994) were used to determine the final values of these parameters, and those reported by others (Adams et al., 1987; Lacroix et al., 2011; Varma et al., 1986) were used to validate them. It should be noted that, during all optimizations, all simulations were adjusted on the basis of dosage and BWs; additionally, every validation was performed immediately following the corresponding optimization. The detailed process of validation is described below.

2.4. Model validation

This model was validated through visual comparisons of the predicted and previously observed FF or FFA concentrations in tissues, plasma, or serum. It is important to emphasize that all of these concentration data for model validations were not applied during the parameter optimizations. The linear regression analysis was also carried out between observations and predictions, and the linear regression determination coefficient was calculated. In addition, the mean absolute percentage error (MAPE) was also calculated according to our previous study (Yang et al., 2018), in which more details about MAPE could be found. The evaluation criteria of MAPE (Lin et al., 2017) are listed as follows: (i) acceptable prediction: MAPE < 50%; (ii) good prediction: 10% < MAPE < 20%; and (iii) excellent prediction: MAPE < 10%.

2.5. Sensitivity analysis

A local sensitivity analysis was performed to determine which parameters were most influential on the area under concentration-time curve (AUC) in plasma, muscle, kidney, and liver for both FF and FFA. During the sensitivity analysis, the central difference method was used and the final value of normalized sensitivity coefficient (NSC) was calculated according to our previous study (Yang et al., 2018). The analysis was performed by using the sensitivity analysis wizard included in the software of acslXtreme. A parameter was considered influential if the absolute value of its NSC was above 0.25 (Leavens et al., 2012). To simultaneously perform the sensitivity analysis for all parameters used in different routes of the model, four routes of administration all at 10 mg/kg BW were simulated simultaneously.

2.6. Monte Carlo analysis

There were up to 50 parameters in this model and the labeled withdrawal period of FF is up to 28 or 38 days in cattle (FARAD, 2002). It would be impossible to subject all parameters to Monte Carlo analysis, because of the computational complexity. Therefore, only the influential parameters (see above sensitivity analysis) were subjected to Monte Carlo analysis. Their central tendency and spread (expressed as average values and SDs) were derived from the previous reports (Doyle et al., 1960; Li et al., 2017; Yang et al., 2013b) or obtained by parameter optimization (see above model parameterization). According to our previous study (Yang et al., 2014), normal distribution was assumed for these parameters, and their distribution information is presented in Table S3. The analysis was performed through the Monte Carlo wizard included in the software of acslXtreme. And one-thousand iterations were simulated for this Monte Carlo analysis. For each simulation, the random numbers for these parameters with the mean value, standard deviation (SD), lower bound (Mean - SD), and upper bound (Mean + SD) were firstly generated by the software of acslXtreme, and then were incorporated into this multiroute model to predict FF and FFA concentrations. Because only IM and SC routes of administration were approved and commonly applied in clinics, both of them were subjected to Monte Carlo analysis. For SC administration, a single dose of FF at 40 mg/kg BW was simulated, while for IM injection, two doses both at 20 mg/kg BW with an interval of 48-h were performed.

2.7. Withdrawal interval estimation

Because of the differences in the marker residues and/or the corresponding MRLs or tolerances adopted by China, US, and UK, the concentrations of FF, FFA, and FF plus FFA were all predicted using the present model. A 1000-iteration Monte Carlo run was further incorporated into this model (see above Monte Carlo analysis). After each run, the predicted concentrations of FF, FFA, and FF plus FFA *versus* time data were all automatically generated by the software of acslXtreme. The Monte Carlo analysis provided all predicted concentrations in 1000 virtual individuals, allowing the withdrawal interval to ensure that the predicted concentrations would be below the corresponding MRL or tolerance to be estimated for each individual. According to the method used in China and EU, the WDI was finally calculated to ensure that the concentrations of total residues of FF plus FFA in 95th percentile of the population were below the MRL, while based on the US method, a 99th percentile was used. Both calculations of WDIs were done by writing an M-type code file in the acslXtreme, which can be found in the Supplementary Materials.

Table 2
The results of optimized parameters used under all routes administration based on the published data.

Optimization order	Routes	Ref. used to optimize parameters	Parameters for FF (unit)	Parameters for FFA (unit)	Initial Value	Final Value	Std. Dev.
1	All	(Bretzlaff et al., 1987) Ref. #1	$Cl_{reperkg}$ (L/h/kg)		0.1	0.5102	0.2839
			P_{re} (unitless)		0.1	1.1332	0.049
			P_{fa} (unitless)		0.1	0.1137	0.0284
			P_{lu} (unitless)		0.1	0.9	0.1231
			K_m (1/h)		0.1	0.2343	0.0498
			K_{mo} (1/h)		0.1	0.1014	0.0267
2	SC	(Kawalek et al., 2016) Ref. #7	K_{asc} (1/h)		0.1	0.1281	0.0102
			F_{sc1} (unitless)		0.2	0.2663	0.0042
			K_{dissc} (1/h)		0.1	0.0054	0.0023
3	All	(Schering-Plough Animal Health Corporation, 2008) Ref. #8		Cl_{mperkg} (L/h/kg)	1E-4	4.5675E-04	1.23E-4
				P_{mli} (unitless)	1	8.7414	1.2013
				P_{mki} (unitless)	1	1.3026	0.3762
				P_{mmu} (unitless)	0.2	0.2778	0.0451
				P_{mre} (unitless)	0.01	0.0121	0.0042
4	IM	(Lobell et al., 1994) Ref. #5	K_{aim} (1/h)		0.1	0.1618	0.032
			F_{im1} (unitless)		0.1	0.4529	0.027
			K_{disim} (1/h)		0.01	0.0104	0.0034
5	PO	(Croubels et al., 2006) Ref. #13	K_{st} (1/h)		0.1	0.1816	0.042
			K_{apo} (1/h)		1	1.9914	0.3082

Note: $Cl_{reperkg}$: renal clearance of FF (normalized by bodyweight); P_{re}, P_{fa}, and P_{lu}: partition coefficients for FF in the rest compartment of body, fat, and lung, respectively; K_m and K_{mo}: transformation rate constants of FFA and all other metabolites from FF, respectively; K_{asc}, K_{aim}, and K_{apo}: absorption rate constants of FF after SC, IM, and PO administration, respectively; K_{st}: rate constant of gastric emptying; K_{dissc} and K_{disim}: distribution rate constants of FF from IS2 to IS1 after SC and IM administration, respectively; F_{sc1} and F_{im1}: fractions of the SC and IM doses allocated to IS1, respectively.

3. Results

3.1. Model parameters

The values of physiological and anatomical parameters used in the present model were derived from a previous model (Li et al., 2017) and are listed in Table 1. The P_xs values of FF in liver, kidney, and muscle were assumed to be equal to those in fish (Yang et al., 2013b), while those in other tissue and all P_{mx}s were obtained through parameter optimization. Their final values were 0.1137, 0.9, and 1.1332 for FF in fat, lung, and rest of body, respectively; while for FFA, the final values were 8.7414, 1.3026, 0.2778, and 0.0121 in liver, kidney, muscle, and rest of body, respectively (Tables 1 and 2). The parameters related to absorption after extravascular administration were also determined through optimization, whose final values were 0.1281 h^{-1}, 0.2663 (unitless), 0.0054 h^{-1}, 0.1618 h^{-1}, 0.4529 (unitless), 0.0104 h^{-1}, 0.1816 h^{-1}, and 1.9914 h^{-1}, for K_{asc}, F_{sc1}, K_{dissc}, K_{aim}, F_{im1}, K_{disim}, K_{st}, and K_{apo}, respectively (Table 2). The other parameters, including $Cl_{reperkg}$, K_m, K_{mo}, and Cl_{mperkg}, were related to the eliminations of FF and FFA, and their values were 0.5102 L/h/kg, 0.2343 h^{-1}, 0.1014 h^{-1}, and 4.5675E-04 L/h/kg, respectively (Table 2).

3.2. Model validation

The multiroute model was validated by visually comparing the predicted and previously published FF or FFA concentrations, and the results are presented in Figs. 1–3 and Figs. S2–S3. As illustrated by these figures, the previously published FF concentrations in serum or plasma after IV and SC injections and those in serum and liver after multiple PO doses were all well predicted, and most of the predicted concentrations are very close to the reported values at the same time points (Figs. 1, S2, and S3B). However, the FF concentrations in plasma were estimated to be approximately 1.5 times higher at later time points after single IM administration (Fig. 3), and similar result can also be found for the predicted FF concentrations in serum after one single PO dose (Fig. S3C). After multiple PO administration, the FF concentrations in lung and muscle were underestimated by approximately 2.5 times (Fig. S3A). For FFA, the liver concentrations at the later time points after a single SC injection were slightly overestimated by 1.5 times (Fig. 2B). Besides visual comparisons, the linear regression analysis was also performed between the predictions and observations, and the results are presented in Table S4. It was shown that the present model was generally acceptable because most of the determination coefficients were higher than 0.75 (a general criterion developed by Li et al. (2018)) except for two values which were 0.7332 and 0.5494 (Table S4). The MAPEs were also calculated to evaluate the present model, whose values ranged from 1.99% to 46.2%, suggesting acceptable predictions for all simulations (Table S4).

3.3. Sensitivity analysis

The complete sensitivity analysis results for all parameters can be found in Tables S5 and S6. An NSC of 1 indicates that there is a one-to-one relationship between the change in the parameter and the AUC, while a negative NSC indicates an inverse relationship between them. The results indicate that most parameters shared the similar extent of impact on the AUCs of FF or FFA in different tissues. However, the parameters of P_{li}, P_{ki}, and P_{mu} only had positive influences on the AUCs of FF in the respective tissues (Table S5). The similar positive impacts on the AUCs of FFA were also observed for the parameters of P_{mli}, P_{mki}, and P_{mmu} (Table S6). The blood flow through lung (Q_{clu}), which was numerically equal to 100% of cardiac output, had the highest impacts on both AUCs of FF and FFA, and this is consistent with the blood flow limited mechanism of the present model.

3.4. Monte Carlo analysis and withdrawal interval estimation

Only the influential parameters were subjected to Monte Carlo analysis. The concentrations of FFA or total residues of FF and FFA after IM and SC routes of administration were predicted based on the Monte Carlo analysis, and the results are presented in Figs. S4 and S5. According to the corresponding tolerances or MRLs, the WDIs of FF were calculated for the population including 1000 virtual individuals, and their distributions are shown in Figs. 4 and 5. After 2 repeated IM injections at 20 mg/kg BW with a 48-h interval, the WDIs calculated based on the marker residue of FFA were 18 and 44 days (99th percentile) in muscle and liver, respectively, while based on the total residue of FF and FFA, they were 23, 41, and 46 days (95th percentile) in muscle, liver, and kidney, respectively (Table 3 and Fig. 4). After one single SC injection of FF at 40 mg/kg BW, the WDIs calculated based on

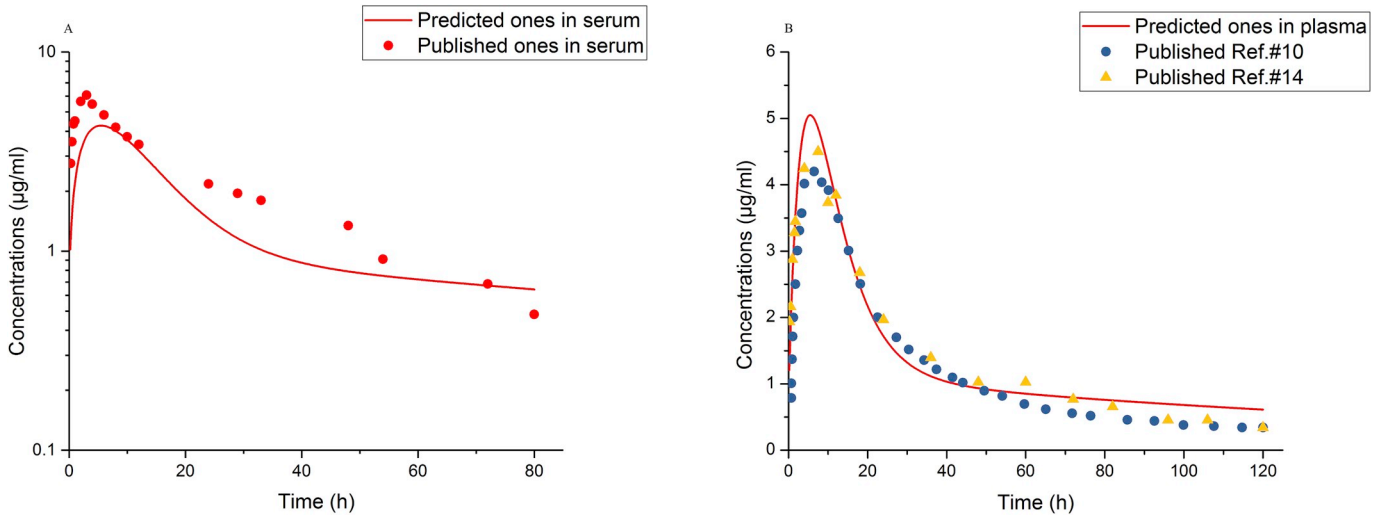

Fig. 1. Comparisons between predicted (curves) and published (points) FF concentrations (μg/ml) in serum (A, Ref#9) and plasma (B, Ref # 10 and 14) after a single SC dose at 40 mg/kg BW in cattle.

FFA concentrations were 20 and 47 days (99th percentile) in muscle and liver, respectively, while those calculated according to total concentrations of FF and FFA were 29, 46, and 58 days (95th percentile) in muscle, liver, and kidney, respectively (Table 3 and Fig. 5).

4. Discussion

Four routes of administration were simulated in this study, including IM, SC, PO and IV administration. The first two are the approved and most commonly used ones for FF to treat bovine respiratory diseases in China, US, and EU; while the latter two routes of administration were also modelled because they can be used to further optimize or validate the current model. As the marker residue of FF, FFA was incorporated into this model together with FF. The FF and FFA submodels were linked through metabolism of FF in liver. To our knowledge, this is the first PBPK model used to simultaneously predict both FF and FFA concentrations in food-producing animals. Population simulation was further incorporated into this model to estimate the WDI needed for FFA or total concentrations of FF and FFA to fall below the corresponding tolerances or MRLs in edible tissues. Based on this model, the concentrations of FF and FFA in cattle plasma, serum, and tissues were predicted after multiple routes of administration, and this model can be further extrapolated to other ruminants, such as goats and sheep.

Compared with the previous PBPK models for FF, the current one has some improvements. The administration routes of IV and SC, as well as the marker residue (FFA) sub-model, were not included in our previous PBPK model in crucian carp (Yang et al., 2013b). Because of the lack of FFA sub-model, WDI was not calculated in the previous model. In addition, the variances of model parameters were not considered in that model, therefore only the average FF concentrations were predicted. Compared with the average model with limited small sample size usually of 25 animals, the population model can provide richer information for a population rather than for an average individual. Another PBPK model was developed for FF in pigs (Qian et al., 2017). In that model, a diffusion-limited compartment was used for lungs to predict FF concentrations in lung interstitial fluid, while flow-limited compartments were used for the other tissues, which is consistent with the current model. However, neither the marker residue FFA nor Monte Carlo simulation was incorporated into the previous pig model; in addition, IM injection was the only available route of administration.

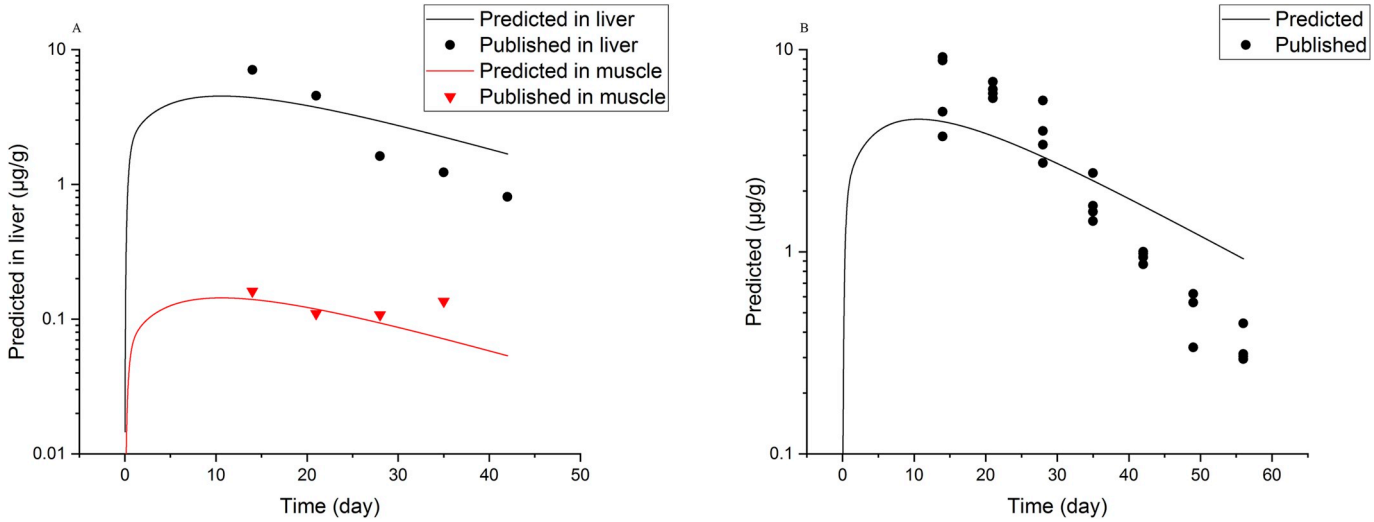

Fig. 2. Comparisons between predicted (curves) and published (points) FFA concentrations (μg/g) in liver and muscle (A, Ref#11) and liver (B, Ref#12) and after a single SC dose at 40 mg/kg in cattle.

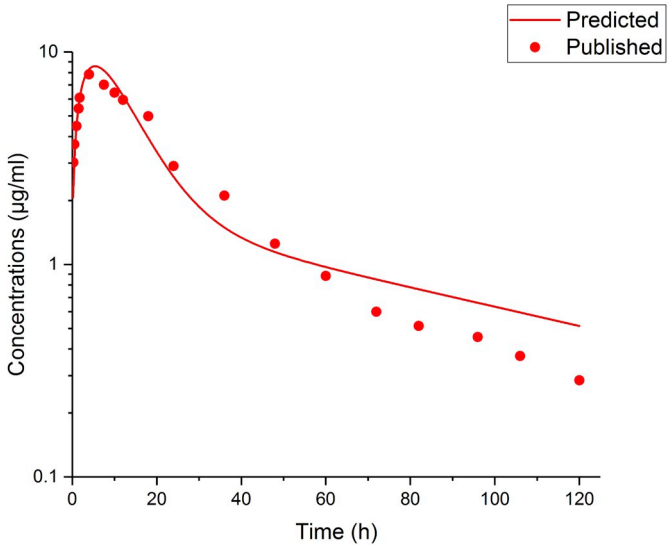

Fig. 3. Comparisons between predicted (curves) and published (points) FF concentrations (μg/ml) in plasma (Ref # 14) after a single IM dose at 40 mg/kg in cattle.

In our previous model in fish (Yang et al., 2013b), the enterohepatic circulation was modelled for FF after oral administration, which was not included in the present one because comparisons between models with or without it through validation showed that it was not an important process in simulating the drug disposition (data not shown). In addition, the simplified structure of the bovine digestive system with multiple stomachs might also impact the simulation of enterohepatic circulation.

In the present model, most of the physiological and anatomical parameters in cattle were derived from a recent cattle PBPK model for penicillin G (Li et al., 2017). Compared to other species, such as rats, dogs, and pigs, there were fewer references about the PBPK model parameters for cattle. Nevertheless, all of these parameters used here were found to be valid because the current model had good predictions in most tissues after different routes of administration. The partition coefficients for FF were assumed to be equal to those previously reported in crucian carp (Yang et al., 2013b) or obtained through parameter optimization with their final values ranging from 0.1137 in fat to 1.3 in liver (Tables 1 and 2), while those for FFA were all obtained by optimization, whose final values ranged from 0.0121 in rest of the body to 8.7414 in liver (Tables 1 and 2). A far higher variance was observed for the partition coefficients for FFA in different tissues compared to those for FF, which demonstrated that FFA residue concentrations might vary greatly in different tissues. All parameters related to the extravascular absorption were obtained by optimization. The values of K_{asc}, K_{aim}, and K_{apo} were optimized to be 0.1281, 0.1618, and 1.9914 h^{-1}, respectively (Table 2), which indicated that the absorption of FF was slower after SC and IM injections than PO administration. Similar slow absorptions after IM and SC injections were also reported for FF in the traditional pharmacokinetic studies in cattle (Lobell et al., 1994; Soback et al., 1995). The parameters related to the elimination were also optimized, whose final values were 0.5102 L/h/kg, 4.5675E-04 L/h/kg, 0.2343 h^{-1}, and 0.1014 h^{-1} for $Cl_{reperkg}$, Cl_{mperkg}, K_m and K_{mo}, respectively (Table 2). It was shown that the elimination of FFA was slower than FF, which was also found in the other species: in sheep (Palma et al., 2012) and fish (Xie et al., 2013), the elimination half-lives of FF were reported as 8.9 and 18.39 h, respectively; while for FFA, they were 17.3 and 25.58 h, respectively. In the present model, the protein binding was not included because of its low extent of binding in cattle (13.2%; Lobell et al., 1994). Therefore, the elimination of FF in this model might be accelerated to some extent. The binding extent for FFA was not available, but due to its structural similarity with FF, it was not considered in the present model, either.

From the validation results, the predictive ability of the PO model was slightly poorer than other routes. This might be due to the assumptions about the bovine digestive system and the absorption process used in this model. In the present study, a virtual compartment was used to simulate the ruminant stomachs, and the drug was assumed to be available immediately after PO administration. However, as indicated by one previous study (Varma et al., 1986), young calves (age

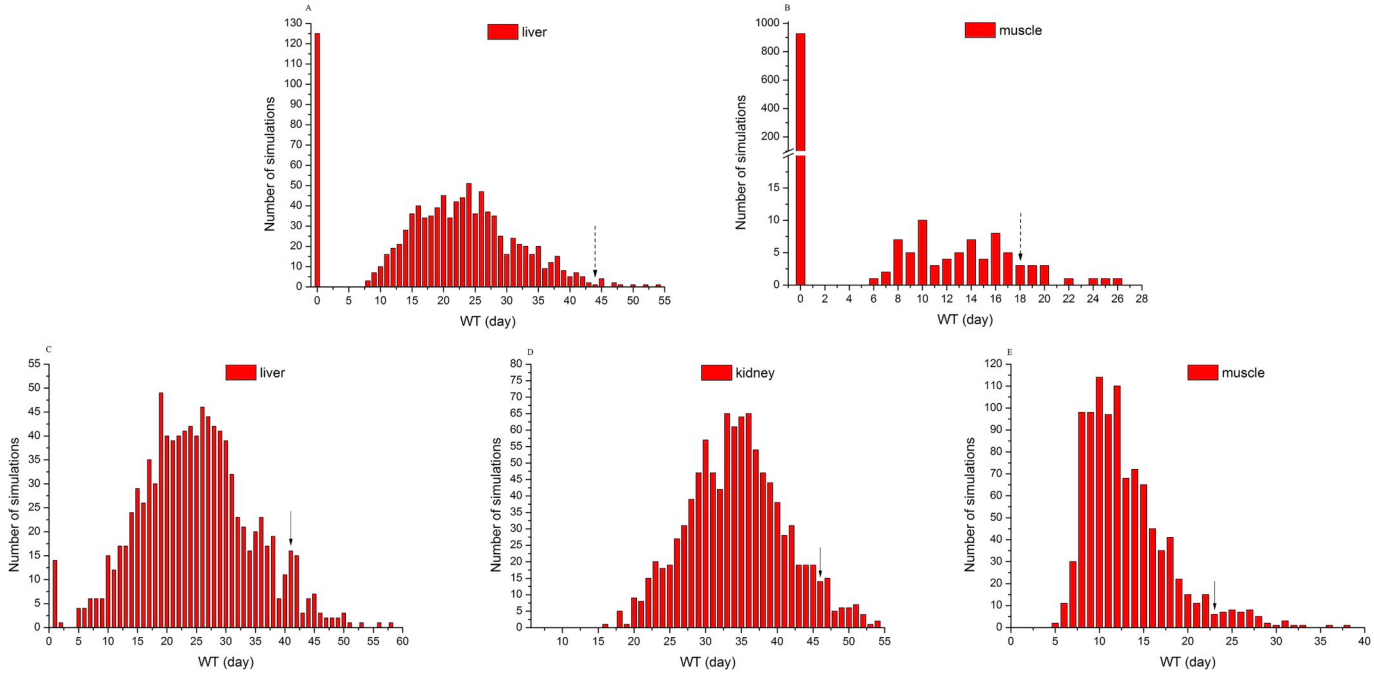

Fig. 4. Distributions of withdrawal intervals after 2 repeated IM injections both at 20 mg/kg BW with an interval of 48 h based on the Monte Carlo analysis: a and b, in liver and muscle, respectively, according to tolerances of FFA; c, d, and e, in liver, kidney, and muscle, respectively, according to MRLs of total residues of FF and FFA. Notes: the solid and dash arrows indicated the 95th and 99th percentiles of the distribution based on Monte Carlo simulation, respectively.

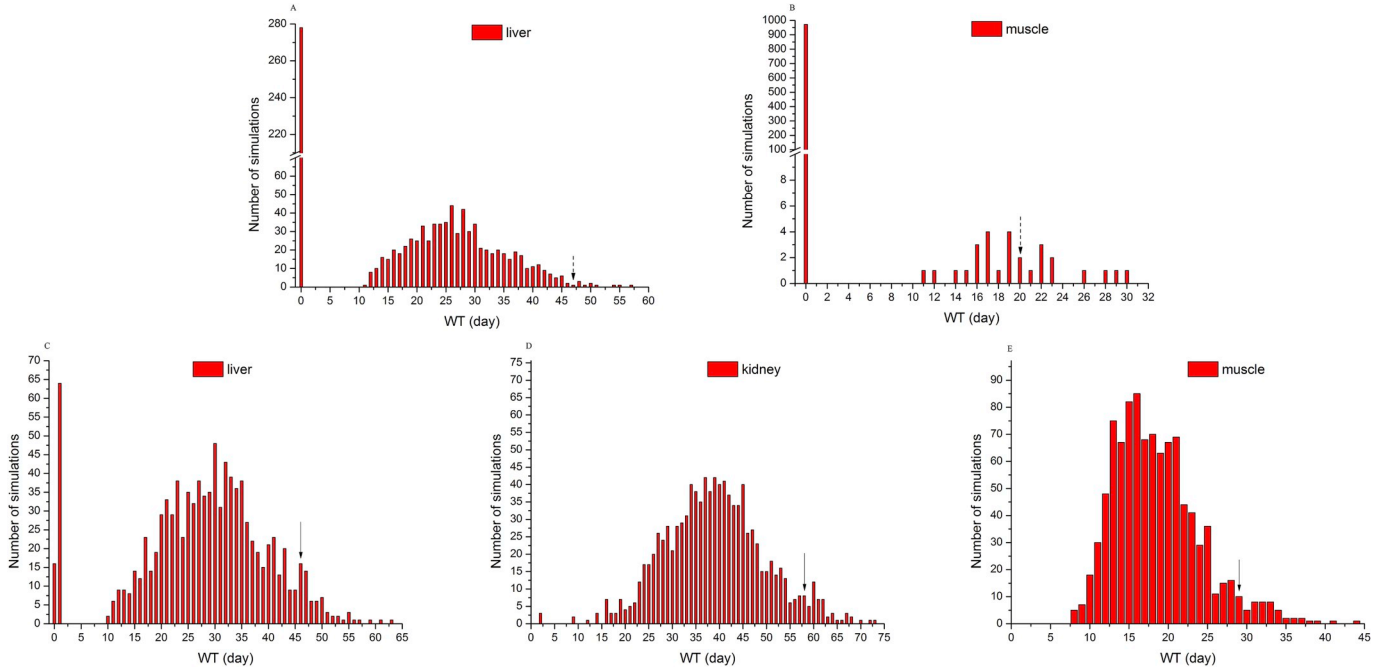

Fig. 5. Distributions of withdrawal intervals after a single SC injection at 40 mg/kg BW based on the Monte Carlo analysis: a and b, in liver and muscle, respectively, according to tolerances of FFA; c, d, and e, in liver, kidney, and muscle, respectively, according to MRLs of total residues of FF and FFA. Notes: the solid and dash arrows indicated the 95th and 99th percentiles of the distribution based on Monte Carlo simulation, respectively.

Table 3
Comparison of the calculated withdrawal intervals (WDI, days) based on the current PBPK model and the labeled withdrawal periods in China, US, and EU.

Tissue	Calculated or labeled WDI based on MRL of FF + FFA						Calculated or labeled WDI based on the tolerance of FFA			
	Calculated values using PBPK model[a]		Labeled values				Calculated values using PBPK model[b]		Labeled values in US	
			In China		In EU					
	IM	SC	IM	SC	IM	SC	IM	SC	IM	SC
muscle	23	29	28	28	30	44	18	20	28	38
Liver	41	46					44	47		
Kidney	46	58					NA	NA		

Note: NA, Not available because of the unavailability of corresponding tolerance in kidney.

[a] These withdrawal intervals were calculated to ensure that the concentrations of total residues of FF plus FFA in 95th percentile of the population were below the corresponding MRLs.

[b] These withdrawal intervals were calculated to ensure that the concentrations of FFA in 99th percentile of the population were below the corresponding tolerances.

1–8 weeks) fed with a milk replacer had a complex absorption pattern with delayed absorption following a single oral dose of FF, and an average lag time was reported as approximately 0.5 h. It is known that young calves may behave more as non-ruminants as their rumen is bypassed. Therefore, in theory, FF may have a longer lag time in adult cattle. We initially tried to incorporate the lag time into the PO model; however, we found that lag time resulted in poor predictions in most tissues, especially in liver and kidney. Given that PO administration was not a common route of administration in clinics and the parameters related to absorption were not influential in this model (Tables S5 and S6), therefore, in the end the lag time was not included in the current model.

There are some limitations to the present study. The first limitation pertains to model validation. In the present model, the FFA concentrations were predicted after all four routes of administration, but the validation was only performed for those after SC administration because of the availability of FFA experimental data. Further studies should be carried out to validate the predicted results for FFA after other routes of administration, especially after IM injection. For the same reason (the unavailability of experimental data), neither the predicted FF nor FFA concentrations in fat were validated here, which should also be further carried out. Secondly, both injection sites after IM and SC administration were included in the present model. However, in order to simplify this model, it was assumed that there were no blood flow. Therefore, the predictions of FFA were not available in the injection site, and the WDIs were not estimated here. For the predictions of FF at the injection site, because of the paucities of the experimental data, these estimates were not validated. Thirdly, during the Monte Carlo simulation, normal distribution was assumed for all influential parameters in the current study. In fact, lognormal distribution was more suitable for the parameters of $Cl_{reperkg}$, Cl_{mperkg}, K_m, and K_{mo} (Li et al., 2017). However, because these parameters were obtained through optimization (Table S3), and only the average values and standard deviations were available for them. Under this circumstance, the lognormal distribution was not able to be used in the software of acslXtreme. Therefore, we finally used the normal distribution for these parameters. Finally, the cattle in the 14 previous studies (Table S1) shared different species, ages or production classes. However, in order to simplify the simulation and because of the paucity of PBPK parameters in different cattle species, only the parameters of BW, tissue weight (expressed as fraction of BW), BW-normalized CO, and blood flow through different tissues (expressed as fraction of CO) were used to simulate different cattle. The differences in age, species, and production classes were not taken into consideration in the present study.

A local sensitivity analysis was performed in the present study. The parameters related to absorption after extravascular administration had less impact on the AUCs of both FF and FFA, which might be because of the relatively slow absorptions of FF. The partition coefficients for FF or FFA in liver, kidney, and muscle were only highly influential on the AUCs of FF or FFA in respective tissues (Tables S5 and S6). The parameters of $Cl_{reperkg}$ and Cl_{mperkg} negatively affected both AUCs of FF and

FFA in all tissues (Tables S5 and S6), while K_m had a positive effect on the AUCs of FFA (Table S6). The parameter of Q_{clu} had the highest impact in the present model, which was consistent with the flow-limited assumption for both FF and FFA. Overall, parameters related to absorption had few effects on the AUCs of both FF and FFA (Tables S5 and S6), and the influential parameters were those related to distribution and elimination of FF and FFA (Tables S5 and S6).

The WDI was calculated using the present population PBPK model with Monte Carlo simulations. Based on the tolerance of FFA adopted by US FDA, the WDIs were calculated as 44- and 47-day for FF after IM (2 repeated doses both at 20 mg/kg BW with an interval of 48 h) and SC (a single dose at 40 mg/kg BW) administration, respectively (Table 3), which were both longer than the US FDA labeled withdrawal periods (28 and 38 days, respectively (FARAD, 2002);). Similarly, the calculated WDI based on the MRLs of FF and FFA was also much longer than those labeled in China and EU (Table 3). One of the challenges associated with current approved methods is the limited number of animals (usually 25 animals) while the Monte Carlo approach allows for 1000 virtual individuals and furthermore not dependent on the descriptive method of the tolerance limit method which relies on the terminal slope to calculate the withdrawal period. The parameter distributions used in our Monte Carlo simulations had a broad range of values and this could have contributed to more conservative estimates of a WDI when compared to the labeled withdrawal times in the various jurisdictions reported in Table 3.

In conclusion, the present model is able to adequately predict the concentrations of FF and FFA after different routes of administration in cattle. The Monte Carlo simulation was incorporated into this model to predict the drug disposition in a population of 1000 individuals and to further estimate the WDIs for FF in cattle after approved label dosing regimens. This study provides a foundation for applying the population PBPK model to predict the residue concentrations of both the parent drug FF and its main metabolite FFA and further estimate the WDI in cattle, which can be extrapolated to other ruminants.

Conflicts of interest

The authors declare no conflict of interest.

Acknowledgements

This study was supported by the National Natural Science Foundation of China (grant No. 31402253 and No. U1604107), China Scholarship Council (grant No. 201608410275), and USDA/NIFA FARAD Program (grant No. 2016-41480-25728).

Appendix A. Supplementary data

Supplementary data to this article can be found online at https://doi.org/10.1016/j.fct.2019.02.029.

Transparency document

Transparency document related to this article can be found online at https://doi.org/10.1016/j.fct.2019.02.029.

References

Adams, P.E., Varma, K.J., Powers, T.E., Lamendola, J.F., 1987. Tissue concentrations and pharmacokinetics of florfenicol in male veal calves given repeated doses. Am. J. Vet. Res. 48 (12), 1725–1732.

Atef, M., El-Gendi, A.Y., Amer, A.M., Abd El-Aty, A.M., 2010. Effect of three anthelmentics on disposition kinetics of florfenicol in goats. Food Chem. Toxicol. 48 (12), 3340–3344.

Baynes, R.E., Dedonder, K., Kissell, L., Mzyk, D., Marmulak, T., Smith, G., Tell, L., Gehring, R., Davis, J., Riviere, J.E., 2016. Health concerns and management of select veterinary drug residues. Food Chem. Toxicol. 88112–88122.

Bretzlaff, K.N., Neff-Davis, C.A., Ott, R.S., Koritz, G.D., Gustafsson, B.K., Davis, L.E., 1987. Florfenicol in non-lactating dairy cows: pharmacokinetics, binding to plasma proteins, and effects on phagocytosis by blood neutrophils. J Vet Pharmacol Ther 10 (3), 233–240.

Buur, J., Baynes, R., Smith, G., Riviere, J., 2006. Use of probabilistic modeling within a physiologically based pharmacokinetic model to predict sulfamethazine residue withdrawal times in edible tissues in swine. Antimicrob. Agents Chemother. 50 (7), 2344–2351.

CCVP, 2015. Veterinary Pharmacopoeia of the People's Republic of China (2015). China Agriculture Press, Beijing.

Croubels, S., Baert, K., Verheyen, T., Boone, G., De Backer, P., 2006. Pharmacokinetics and oral bioavailability of florfenicol in veal calves. J Vet Pharmacol Ther 29 (Suppl. 1), 278–279.

de Craene, B.A., Deprez, P., D'Haese, E., Nelis, H.J., Van den Bossche, W., De Leenheer, P., 1997. Pharmacokinetics of florfenicol in cerebrospinal fluid and plasma of calves. Antimicrob. Agents Chemother. 41 (9), 1991–1995.

Doyle, J.T., Patterson Jr., J.L., Warren, J.V., Detweiler, D.K., 1960. Observations on the circulation of domestic cattle. Circ. Res. 84–15.

EMA, 1996. Committee for veterinary medicinal products Florfenicol Summary report (1). http://www.ema.europa.eu/docs/en_GB/document_library/Maximum_Residue_Limits_-_Report/2009/11/WC500014274.pdf, Accessed date: 14 September 2018.

EMA, 1997. Committee for veterinary medicinal products Florfenicol (Extension to fish) Summary report (2). http://www.ema.europa.eu/ema/pages/includes/document/open_document.jsp?webContentId=WC500014279, Accessed date: 14 September 2018.

EMA, 2002. Committee for veterinary medicinal products Florfenicol (Extension to all food producing species) Summary report (6). http://www.ema.europa.eu/docs/en_GB/document_library/Maximum_Residue_Limits_-_Report/2009/11/WC500014282.pdf, Accessed date: 14 September 2018.

FARAD, 2002. Approved food animal drugs. http://www.farad.org/vetgram/ProductInfo.asp, Accessed date: 14 September 2018.

FDA, 2017. Title 21–food and drugs chapter I–Food and drug administration sec. 556.283 florfenicol. https://www.accessdata.fda.gov/scripts/cdrh/cfdocs/cfcfr/CFRSearch.cfm?fr=556.283, Accessed date: 14 September 2018.

FDA, 2018. Guidance for industry #3, general principles for evaluating the human food safety of new animal drugs used in food-producing animals. https://www.fda.gov/downloads/AnimalVeterinary/GuidanceComplianceEnforcement/GuidanceforIndustry/ucm052180.pdf, Accessed date: 18 September 2018.

Gilliam, J.N., Streeter, R.N., Papich, M.G., Washburn, K.E., Payton, M.E., 2008. Pharmacokinetics of florfenicol in serum and synovial fluid after regional intravenous perfusion in the distal portion of the hind limb of adult cows. Am. J. Vet. Res. 69 (8), 997–1004.

Hendrick, S.H., Bateman, K.G., Rosengren, L.B., 2013. The effect of antimicrobial treatment and preventive strategies on bovine respiratory disease and genetic relatedness and antimicrobial resistance of *Mycoplasma bovis* isolates in a western Canadian feedlot. Can. Vet. J. 54 (12), 1146–1156.

Henri, J., Carrez, R., Meda, B., Laurentie, M., Sanders, P., 2017. A physiologically based pharmacokinetic model for chickens exposed to feed supplemented with monensin during their lifetime. J Vet Pharmacol Ther 40 (4), 370–382.

Intervet Inc, 2009. Freedom of Information Summary: original new animal drug application, NADA 141-299, Resflor gold: florfenicol and flunixin meglumine (in 2-pyrrolidone and triacetin) injectable solution beef and non-lactating dairy cattle. http://cafarad.ucdavis.edu/citationsearch/SearchCitations/9014087.pdf, Accessed date: 30 October 2017.

Kawalek, J.C., Howard, K.D., Jones, Y., Scott, M.L., Myers, M.J., 2016. Depletion of florfenicol in lactating dairy cows after intramammary and subcutaneous administration. J Vet Pharmacol Ther 39 (6), 602–611.

Klein, U., de Jong, A., Moyaert, H., El Garch, F., Leon, R., Richard-Mazet, A., Rose, M., Maes, D., Pridmore, A., Thomson, J.R., Ayling, R.D., 2017. Antimicrobial susceptibility monitoring of *Mycoplasma hyopneumoniae* and *Mycoplasma bovis* isolated in Europe. Vet. Microbiol. 204, 188–193.

Klima, C.L., Alexander, T.W., Hendrick, S., McAllister, T.A., 2014. Characterization of *Mannheimia haemolytica* isolated from feedlot cattle that were healthy or treated for bovine respiratory disease. Can. J. Vet. Res. 78 (1), 38–45.

Lacroix, M.Z., Gayrard, V., Picard-Hagen, N., Toutain, P.L., 2011. Comparative bioavailability between two routes of administration of florfenicol and flunixin in cattle. Rev. Med. Vet. (Toulouse) 162 (6), 321–324.

Lamm, C.G., Love, B.C., Krehbiel, C.R., Johnson, N.J., Step, D.L., 2012. Comparison of antemortem antimicrobial treatment regimens to antimicrobial susceptibility patterns of postmortem lung isolates from feedlot cattle with bronchopneumonia. J. Vet. Diagn. Invest. 24 (2), 277–282.

Leavens, T.L., Tell, L.A., Clothier, K.A., Griffith, R.W., Baynes, R.E., Riviere, J.E., 2012. Development of a physiologically based pharmacokinetic model to predict tulathromycin distribution in goats. J Vet Pharmacol Ther 35 (2), 121–131.

Leavens, T.L., Tell, L.A., Kissell, L.W., Smith, G.W., Smith, D.J., Wagner, S.A., Shelver, W.L., Wu, H., Baynes, R.E., Riviere, J.E., 2014. Development of a physiologically based pharmacokinetic model for flunixin in cattle (*Bos taurus*). Food Addit. Contam. Part A Chem Anal Control Expo Risk Assess 31 (9), 1506–1521.

Li, Y.F., Zhao, N., Zeng, Z.L., Gu, X.Y., Fang, B.H., Yang, F., Zhang, B.X., Ding, H.Z., 2013. Tissue deposition and residue depletion of cyadox and its three major metabolites in pigs after oral administration. J. Agric. Food Chem. 61 (39), 9510–9515.

Li, M., Gehring, R., Riviere, J.E., Lin, Z., 2017. Development and application of a population physiologically based pharmacokinetic model for penicillin G in swine and cattle for food safety assessment. Food Chem. Toxicol. 107 (Pt A), 74–87.

Li, M., Gehring, R., Riviere, J.E., Lin, Z., 2018. Probabilistic physiologically based pharmacokinetic model for Penicillin G in milk from dairy cows following intramammary or intramuscular administrations. Toxicol. Sci. 164 (1), 85–100.

Lin, Z., Gehring, R., Mochel, J.P., Lave, T., Riviere, J.E., 2016. Mathematical modeling and simulation in animal health - Part II: principles, methods, applications, and value of physiologically based pharmacokinetic modeling in veterinary medicine and food safety assessment. J Vet Pharmacol Ther 39 (5), 421–438.

Lin, Z., Jaberi-Douraki, M., He, C., Jin, S., Yang, R.S.H., Fisher, J.W., Riviere, J.E., 2017. Performance assessment and translation of physiologically based pharmacokinetic models from acslX to Berkeley Madonna, MATLAB, and R language: oxytetracycline and gold Nanoparticles as Case Examples. Toxicol. Sci. 158 (1), 23–35.

Liu, X., Steele, J.C., Meng, X.Z., 2017. Usage, residue, and human health risk of antibiotics in Chinese aquaculture: a review. Environ. Pollut. 223, 161–169.

Lobell, R.D., Varma, K.J., Johnson, J.C., Sams, R.A., Gerken, D.F., Ashcraft, S.M., 1994. Pharmacokinetics of florfenicol following intravenous and intramuscular doses to cattle. J Vet Pharmacol Ther 17 (4), 253–258.

Norbrook Laboratories, Ltd, 2015. Freedom of information summary: original abbreviated new animal drug application NADA 200-591 NORFENICOL florfenicol injectable solution beef and non-lactating dairy cattle. http://cafarad.ucdavis.edu/citationsearch/SearchCitations/9016669.pdf, Accessed date: 25 October 2017.

Palma, C., Ramirez, J., Benavente, A., Cazanga, V., Venegas, M., Perez, R., 2012. Pharmacokinetics of florfenicol and florfenicol-amine after intravenous administration in sheep. J Vet Pharmacol Ther 35 (5), 508–511.

Qian, M.R., Wang, Q.Y., Yang, H., Sun, G.Z., Ke, X.B., Huang, L.L., Gao, J.D., Yang, J.J., Yang, B., 2017. Diffusion-limited PBPK model for predicting pulmonary pharmacokinetics of florfenicol in pig. J Vet Pharmacol Ther 40 (6), e30–e38.

Riviere, J.E., Tell, L.A., Baynes, R.E., Vickroy, T.W., Gehring, R., 2017. Guide to FARAD resources: historical and future perspectives. J. Am. Vet. Med. Assoc. 250 (10), 1131–1139.

Schering-Plough Animal Health Corporation, 2006. Freedom of Information Summary, Supplemental New Animal Drug Application NADA 141-063, Nuflor Injectable Solution, Forfenicol Injectable Solution. Cattle. US FDA. http://cafarad.ucdavis.edu/citationsearch/SearchCitations/9014514.pdf, Accessed date: 25 October 2017.

Schering-Plough Animal Health Corporation, 2008. Freedom of information summary: original new animal drug application, NADA 141-265. Nuflor gold injectable solution. Florfenicol (with 2-pyrrolidone and triacetin). Beef and non-lactating dairy cattle. http://cafarad.ucdavis.edu/citationsearch/SearchCitations/9014686.pdf, Accessed date: 25 October 2017.

Sidhu, P., Rassouli, A., Illambas, J., Potter, T., Pelligand, L., Rycroft, A., Lees, P., 2014. Pharmacokinetic-pharmacodynamic integration and modelling of florfenicol in calves. J Vet Pharmacol Ther 37 (3), 231–242.

Soback, S., Paape, M.J., Filep, R., Varma, K.J., 1995. Florfenicol pharmacokinetics in lactating cows after intravenous, intramuscular and intramammary administration. J Vet Pharmacol Ther 18 (6), 413–417.

Thiry, J., Gonzalez-Martin, J.V., Elvira, L., Pagot, E., Voisin, F., Lequeux, G., Weingarten, A., de Haas, V., 2014. Treatment of naturally occurring bovine respiratory disease in juvenile calves with a single administration of a florfenicol plus flunixin meglumine formulation. Vet. Rec. 174 (17), 430.

Timsit, E., Hallewell, J., Booker, C., Tison, N., Amat, S., Alexander, T.W., 2017. Prevalence and antimicrobial susceptibility of *Mannheimia haemolytica, Pasteurella multocida*, and *Histophilus somni* isolated from the lower respiratory tract of healthy feedlot cattle and those diagnosed with bovine respiratory disease. Vet. Microbiol. 208, 118–125.

Varma, K.J., Adams, P.E., Powers, T.E., Powers, J.D., Lamendola, J.F., 1986. Pharmacokinetics of florfenicol in veal calves. J Vet Pharmacol Ther 9 (4), 412–425.

Veterinary Medicines Directorate, 2007. Product information database. http://www.vmd.defra.gov.uk/ProductInformationDatabase/Default.aspx, Accessed date: 17 September 2018.

Wang, Z., Kong, L., Jia, B., Liu, S., Ma, H., 2015. Isolation, identification and resistance analysis of seven capsular serotype A *Pasteurella multocida*. Chinese Journal of Veterinary Drug 49 (7), 8–12.

Welsh, R.D., Dye, L.B., Payton, M.E., Confer, A.W., 2004. Isolation and antimicrobial susceptibilities of bacterial pathogens from bovine pneumonia: 1994–2002. J. Vet. Diagn. Invest. 16 (5), 426–431.

Xie, L.L., Wu, Z.X., Chen, X.X., Li, Q., Yuan, J., Liu, H., Yang, Y., 2013. Pharmacokinetics of florfenicol and its metabolite, florfenicol amine, in rice field eel (*Monopterus albus*) after a single-dose intramuscular or oral administration. J Vet Pharmacol Ther 36 (3), 229–235.

Yang, F., Liu, H.W., Li, M., Ding, H.Z., Huang, X.H., Zeng, Z.L., 2012. Use of a Monte Carlo analysis within a physiologically based pharmacokinetic model to predict doxycycline residue withdrawal time in edible tissues in swine. Food Addit. Contam. Part A Chem Anal Control Expo Risk Assess 29 (1), 73–84.

Yang, F., Huang, X.H., Li, G.H., Ni, H.J., Zhao, Y.D., Ding, H.Z., Zeng, Z.L., 2013a. Estimating tulathromycin withdrawal time in pigs using a physiologically based pharmacokinetics model. Food Addit. Contam. Part A Chem Anal Control Expo Risk Assess 30 (7), 1255–1263.

Yang, F., Sun, N., Sun, Y.X., Shan, Q., Zhao, H.Y., Zeng, D.P., Zeng, Z.L., 2013b. A physiologically based pharmacokinetics model for florfenicol in crucian carp and oral-to-intramuscular extrapolation. J Vet Pharmacol Ther 36 (2), 192–200.

Yang, F., Yang, Y.R., Wang, L., Huang, X.H., Qiao, G., Zeng, Z.L., 2014. Estimating marbofloxacin withdrawal time in broiler chickens using a population physiologically based pharmacokinetics model. J Vet Pharmacol Ther 37 (6), 579–588.

Yang, F., Sun, N., Liu, Y.M., Zeng, Z.L., 2015. Estimating danofloxacin withdrawal time in broiler chickens based on physiologically based pharmacokinetics modeling. J Vet Pharmacol Ther 38 (2), 174–182.

Yang, F., Si, H.B., Wang, Y.Q., Zhao, Z.S., Zhou, B.H., Hao, X.Q., 2016. Pharmacokinetics of doxycycline in laying hens after intravenous and oral administration. Br. Poult. Sci. 57 (4), 576–580.

Yang, F., Yang, F., Shi, W., Si, H., Kong, T., Wang, G., Zhang, J., 2018. Development of a multiroute physiologically based pharmacokinetic model for orbifloxacin in rabbits. J Vet Pharmacol Ther 41 (4), 622–631.

Zeng, D., Lin, Z., Fang, B., Li, M., Gehring, R., Riviere, J.E., Zeng, Z., 2017. Pharmacokinetics of mequindox and its marker residue 1,4-bisdesoxymequindox in swine following multiple oral gavage and intramuscular administration: an experimental study coupled with population physiologically based pharmacokinetic modeling. J. Agric. Food Chem. 65 (28), 5768–5777.

Zhu, X., Huang, L., Xu, Y., Xie, S., Pan, Y., Chen, D., Liu, Z., Yuan, Z., 2017. Physiologically based pharmacokinetic model for quinocetone in pigs and extrapolation to mequindox. Food Addit. Contam. Part A Chem Anal Control Expo Risk Assess 34 (2), 192–210.